(4) R. D. Adams and F. A. Cotton, *J. Am. Chem. Soc.*, **95**, 6589 (1973).

(5) F. A. Cotton, Plenary Lecture, Assemblee Annuelle, Societe Chimique de France, Marseille, May 22–25, 1972; *Bull. Soc. Chim. Fr.*, 2588 (1973).

(6) F. A. Cotton, Plenary Lecture, 6th International Conference on Organometallic Chemistry, Amherst, Mass., Aug 13, 1973; see Abstracts, pp 1–8.

(7) R. D. Adams and F. A. Cotton, "Dynamic Nuclear Magnetic Resonance Spectroscopy", L. Jackman and F. A. Cotton, Ed., Academic Press, New York, N.Y., 1975, Chapter 12, especially pp 509–510.

(8) R. D. Adams, M. D. Brice, and F. A. Cotton, *Inorg. Chem.*, **13**, 1080 (1974).

(9) F. A. Cotton, L. Kruczynski, and A. J. White, *Inorg. Chem.*, **13**, 1402 (1974).

(10) D. C. Harris, E. Rosenberg, and J. D. Roberts, *J. Chem. Soc., Dalton Trans.*, 2398 (1974).

(11) E. Weiss and W. Hubel, *Chem. Ber.*, **95**, 1186 (1962).

(12) R. B. King, *J. Am. Chem. Soc.*, **88**, 2075 (1966).

(13) M. R. Churchill and P. H. Bird, *Inorg. Chem.*, **8**, 1941 (1969).

(14) G. Crane, G. E. Boord, and A. L. Henne, *J. Am. Chem. Soc.*, **67**, 1237 (1945).

(15) R. Burton, L. Pratt, and G. Wilkinson, *J. Chem. Soc.*, 4290 (1960).

(16) M. R. Churchill, *Inorg. Chem.*, **6**, 190 (1967).

(17) All necessary references to sources of data and computer programs used will be found in F. A. Cotton and P. Lahuerta, *Inorg. Chem.*, **14**, 116 (1975).

(18) Supplementary data.

(19) O. A. Gansow, A. R. Burke, and W. D. Vernon, *J. Am. Chem. Soc.*, **94**, 2550 (1972); F. A. Cotton, D. L. Hunter, and A. J. White, *Inorg. Chem.*, **14**, 703 (1975).

(20) J. W. Emsley, J. Feeney, and L. H. Sutcliffe, "High Resolution Nuclear Magnetic Resonance Spectroscopy," Vol. 1, Pergamon Press, Oxford, 1965, Chapter 9.

(21) J. Takats and L. Kruczynski, *J. Am. Chem. Soc.*, **96**, 932 (1974).

(22) J.-Y. Lallemand, P. Lazlo, C. Muzette, and A. Stockis, *J. Organomet. Chem.*, **91**, 71 (1975).

(23) K. Noack, *J. Inorg. Nucl. Chem.*, **25**, 1383 (1963).

(24) A. R. Manning, *J. Chem. Soc. A*, 1319 (1968).

(25) P. McArdle, A. R. Manning, and F. S. Stephens, *Chem. Commun.*, 1310 (1969).

(26) F. S. Stephens, *J. Chem. Soc. A*, 1722 (1970).

(27) We expressly emphasize that this conclusion is being drawn with reference to this class of iron compounds only, and not necessarily any more widely. In fact it has recently been shown[28] that a direct 1 for 1 switching mechanism does occur in $(\eta^5\text{-}C_5H_5)_2Rh_2(CO)_2P(OPh)_3$.

(28) J. Evans, B. F. G. Johnson, J. Lewis, and T. W. Matheson, *J. Chem. Soc., Chem. Commun.*, 576 (1975).

Contribution from the Department of Chemistry,
University of Minnesota, Minneapolis, Minnesota 55455

Oxidation of Tris(*N*,*N*-disubstituted-dithiocarbamato) Complexes of Ruthenium(III). X-Ray Structure Determination of Bis(*N*,*N*-diethyldithiocarbamato)-*μ*-tris(*N*,*N*-diethyldithiocarbamato)-diruthenium(III) Tetrafluoroborate, $[Ru_2(Et_2dtc)_5]BF_4$

B. M. MATTSON, J. R. HEIMAN, and L. H. PIGNOLET*

Received November 5, 1975 AIC507965

The products of the oxidation reaction of tris(*N*,*N*-disubstituted-dithiocarbamato)ruthenium(III), $Ru(R_2dtc)_3$, with BF_3 gas open to the air have been characterized by standard analytical and spectroscopic means. The novel metal-containing product has the formula $[Ru_2(R_2dtc)_5]BF_4$ and the crystal structure has been determined for R = ethyl by three-dimensional single-crystal x-ray analysis. The space group is $Pna2_1$ with lattice constants $a = 18.303$ (6) Å, $b = 20.713$ (9) Å, and $c = 12.416$ (5) Å. The structure was solved by conventional heavy-atom techniques and refined by least-squares methods to weighted and unweighted R factors of 0.089 and 0.095, respectively, for 2100 independent reflections. The density of 1.54 g/cm^3 computed from the unit cell volume of 4707 Å^3 on the basis of four $[Ru_2(Et_2dtc)_5]BF_4{\cdot}C_3H_6O$ molecules per unit cell agrees well with the 1.55 g/cm^3 determined by flotation methods. The structure of the cation consists of a triply bridged diruthenium compound (see Figures 1–3) with a Ru–Ru distance of 2.743 (3) Å. This distance and the diamagnetism of the compound are consistent with a bond order equal to ~1. The structure is novel because it is the first example where dithiocarbamate ligands connect two metals in both bridging fashions simultaneously. The mechanism of the oxidation reaction is discussed and compared to the analogous reaction of $Fe(R_2dtc)_3$ which gives a monomeric tris-chelate complex of iron(IV). A thorough electrochemical study has also been carried out on $Ru(R_2dtc)_3$ and $[Ru_2(R_2dtc)_5]BF_4$ complexes.

Introduction

Recently it has been shown that the *N*,*N*-disubstituted-dithiocarbamato ligand, R_2dtc^-, can stabilize metals in unusually high oxidation states including Cu(III),[1] Ni(IV),[1-4] Fe(IV),[5-10] Mn(IV),[11-13] Co(IV),[5,13] Pd(IV),[4,14] and Pt(IV).[4,14] For example, the reaction of $Fe(R_2dtc)_3$ complexes, where R = alkyl or aryl, with oxidizing agents such as $Fe(ClO_4)_3{\cdot}6H_2O$ or BF_3 gas open to the air gives stable paramagnetic tris-chelate complexes of Fe(IV),[5-10] $[Fe(R_2dtc)_3]X$, where $X^- = ClO_4^-$ or BF_4^-, respectively. One of these Fe(IV) complexes, $R_2 = (CH_2)_4$, has been shown by x-ray crystallography[8] to be monomeric with no evidence for intra- or interligand oxidation to a disulfide linkage. Similar results have been obtained for $\{Mn[(CH_2)_5dtc]_3\}ClO_4$[11,12] and $\{Ni[(n\text{-}C_4H_9)_2dtc]_3\}Br$[2] by x-ray analysis.

The oxidation reaction using BF_3 gas under aerobic conditions has very recently been carried out on $M(R_2dtc)_3$ complexes of Co(III), Rh(III), and Ru(III) to give diamagnetic products.[15] Monomeric tris-chelate complexes of Co(IV) and Rh(IV) (d^5), and Ru(IV) (d^4) are expected to be paramagnetic. Indeed, a recent report[13] claims evidence for $[Co(R_2dtc)_3]BF_4$ where R = cyclohexyl which has a magnetic moment of 3.48 BM.[16] It is now firmly established that the diamagnetic cobalt oxidation product has the stoichiometry $[Co_2(R_2dtc)_5]BF_4$ and that the diamagnetism results from the low-spin d^6 Co(III) ion.[17] The rhodium and ruthenium complexes presumably have the same stoichiometry. It is interesting that with these metals the ligand and not the metal is oxidized. A recent polarographic study[18] showed that the one-electron oxidation half-wave potentials for $M(Et_2dtc)_3$[19] in DMF where M = Fe(III) and Ru(III) are +0.423 and +0.382 V vs. sce, respectively. In view of the similarity of these potentials and the apparent difference in the structures of oxidation product, $[Fe(Et_2dtc)_3]BF_4$ vs. $[Ru_2(Et_2dtc)_5]BF_4$, a complete characterization and x-ray investigation of the ruthenium oxidation product have been carried out. A preliminary account of this work has been published.[20]

Experimental Section

Synthesis of $[Ru_2(R_2dtc)_5]BF_4$ Complexes. The complexes with R = methyl, ethyl, or benzyl and R_2 = pyrrolidyl were synthesized by oxidation of the respective tris chelates, $Ru(R_2dtc)_3$, according to the method of Pasek and Straub.[5] For example, boron trifluoride gas was slowly bubbled through a benzene solution of $Ru(Et_2dtc)_3$[21]

Table I. Characterization Data for $[Ru_2(R_2dtc)_5]BF_4$ Complexes

	Elemental analysis[a]						Mol wt ($CHCl_3$ soln)		Ir,[c] ν(C$\overset{...}{-}$N) (KBr disk) cm^{-1}	Equiv conductance,[d] mhos cm^2 $equiv^{-1}$
	% C		% H		% N					
R	Calcd	Found	Calcd	Found	Calcd	Found	Calcd	Found		
CH_3	20.24	20.20	3.40	3.49	7.87	7.89	890	*b*	1544	74
C_2H_5	29.15	29.21	4.82	4.91	6.80	5.95	1030	1090	1513	90
$CH_2C_6H_5$	54.56	52.30	4.27	4.70			1580	1353	1496	68
$(CH_2)_4$	29.43	29.67	3.95	4.55	6.87	5.51	1020	1076	1502	98

[a] These compounds were difficult to analyze which accounts for the rather large disagreement in several cases. [b] Insoluble. [c] The C–N stretching region is broad and the number reported corresponds to the point of maximum absorption. [d] Nitromethane solution at 25°C. Comparison data for $Fe(R_2dtc)_3BF_4$ complexes[5] where R = CH_3, C_2H_5, $(CH_2)_4$: 95, 87, 95 mhos cm^2/equiv, respectively.

Table II. Crystal Data for $Ru_2[S_2CN(C_2H_5)_2]_5BF_4\cdot C_3H_6O$[a]

Fw 1088
$a = 18.303\ (6)$ Å
$b = 20.713\ (9)$ Å
$c = 12.416\ (5)$ Å
$\alpha = \beta = \gamma = 90°$
$V = 4707$ Å^3

Orthorhombic
Space group $Pna2_1$
Mo Kα radiation
$\mu = 11.0\ cm^{-1}$
$d_{calcd} = 1.54\ g\ cm^{-3}$ ($Z = 4$)
$d_{obsd} = 1.55\ g\ cm^{-3}$ [b]

[a] The numbers in parentheses in this and succeeding tables represent the estimated standard deviation of the last significant figure(s). [b] Determined by flotation from iodomethane–petroleum ether solvent mixtures.

(ca. 0.5 g in ca. 50 ml) open to the air, for ca. 20 s with stirring. A dark red oil separated which was initially purified by decanting off the clear benzene solution and washing thoroughly with benzene and petroleum ether. A pure product is obtained by column chromatography from silica gel using a CH_2Cl_2–acetone solvent mixture (70:30 v/v) as eluent. The first band was collected and concentrated and a crystalline product was obtained by slow evaporation from methylene chloride–heptane or diethyl ether–acetone solvent mixtures. All four complexes were synthesized in an identical manner. The complexes were found to be pure by elemental analysis, thin-layer chromatography, and proton magnetic resonance spectroscopy (see Table I). Characteristic infrared data (KBr disk) in the range 2000–700 cm^{-1} are for R = Et 1526 sh, s, 1513 s, 1460 m, 1440 m, 1420 w, 1381 w, 1356 m, 1279 s, 1207 m, 1449 m, 1053 br, s, 995 sh, m, 910 w, 849 w, 777 cm^{-1} w.

Structure Determination. Single crystals of $[Ru_2(Et_2dtc)_5]BF_4\cdot C_3H_6O$ were grown by slow evaporation from a diethyl ether–acetone solvent mixture (ca. 50:50 v/v). The crystals were very fragile and contained acetone of solvation as determined by ^1H NMR and chemical ionization mass spectroscopy. The crystal which was used for data collection was a rectangular needle and had dimensions 0.17 × 0.17 × 0.63 mm^3, elongated parallel to *c*. The *c* axis was parallel to the spindle axis. The mounted crystal was coated with 5-min epoxy resin to minimize solvent loss.

The systematic absences were obtained from precession film data (Cu Kα radiation) and are $0kl$ ($k + l = 2n$), $h0l$ ($h = 2n$), $h00$ ($h = 2n$), $0k0$ ($k = 2n$), and $00l$ ($l = 2n$) which indicate the space group to be $Pna2_1$. This space group was used for solution and refinement of the structure. The unit cell dimensions were determined by least-squares refinement using the θ angle values for 12 Mo Kα (λ 0.7107 Å) peaks scanned with a diffractometer at room temperature. The crystal data are reported in Table II.

Intensity data were collected at room temperature on a four-circle Hilger and Watts automatic diffractometer. The incident beam was Zr-filtered Mo Kα radiation. The scan was eighty 0.01° steps in θ and ω from −0.40 to +0.40° with respect to the calculated setting. The step time was 1 s and the background was counted for 20 s at each limit of the scan while crystal and counter were stationary. The counting times were tripled for $\theta > 18°$. A total of 2941 independent reflections were collected over one octant for θ between 0 and 21°. The number of nonzero reflections (i.e., with $F_o^2 > 2.5\sigma(F_o^2)$) used in the structure determination was 2100. Two standard reflection intensities were checked at intervals of 25 sequential reflections. A 30% decay of the initial intensities of both standard reflections was observed during data collection and attributed to decomposition. Scale factors were adjusted on the assumption that all reflections decreased at the same rate.

The data were processed in the manner described by Corfield, Doedens, and Ibers;[22] the value of 0.03 was used for p in the $\sigma(I)$ equation. The intensity data were corrected for Lorentz and polarization effects and for absorption ($\mu = 10.98\ cm^{-1}$) using the program DATAP2.[23] A grid size of 4 × 4 × 4 was used for the absorption correction.

The two ruthenium and several sulfur atoms were located from a three-dimensional Patterson map.[24] Subsequent three-dimensional Fourier maps, phased by the ruthenium atoms and observed sulfur atoms, eventually showed most of the carbon and nitrogen atoms. Several cycles of full-matrix least-squares refinement with 35 of the 42 atoms of the cation included yielded $R_1 = 0.16$.[25] The remaining carbon atoms and two large areas of electron density presumed to be the BF_4 anion and the acetone of solvation were located in a difference Fourier map. At this point in the refinement the two ruthenium and ten sulfur atoms were allowed to be thermally anisotropic, the four fluorine atoms were included at the regions of maximum electron density approximating a tetrahedron, and two carbon atoms called X(1) and X(2) were included at points of maximum electron density in the acetone region. Three cycles of full-matrix least-squares refinement yielded $R_1 = 0.11$. A difference Fourier and the large thermal parameters observed for the fluorine and acetone carbon atoms showed significant disorder in these atoms. Several attempts to improve the fit were unsuccessful. Finally, it was decided to allow the four fluorine atoms, the two acetone carbon positions, and all ten methyl carbon atoms to be thermally anisotropic. The boron atom was placed in the center of the four fluorine positions and not refined. Three more cycles of full-matrix least-squares refinement yielded $R_1 = 0.098$; however, several of the terminal methyl carbons, the four fluorine atoms, and the two acetone positions had large thermal parameters. A difference Fourier showed some residual electron density near the BF_4 and acetone regions. Three final cycles of full-matrix least-squares refinement with the two ruthenium, ten sulfur, ten terminal methyl carbon, four fluorine, and two acetone carbon atoms thermally anisotropic were performed with the boron, four fluorine, and two acetone carbon atoms not refined. The final agreement factors are $R_1 = 0.095$ and $R_2 = 0.089$.[26] Further refinement was not attempted for the following reasons: (i) all of the full shifts in the thermal and positional parameters for the refined atoms in the last cycle of least-squares refinement were much less than the standard deviations; (ii) the chemically sought information, i.e., the distances and angles within the Ru_2S_{10} core and the overall structure of the cation was obtainable and not significantly affected by the disorder. Conductivity, ^1H NMR, chemical ionization mass spectroscopy, molecular weight determination, and elemental analysis confirmed the stoichiometry as $Ru_2(Et_2dtc)_5BF_4\cdot C_3H_6O$ which eliminated the possibility of incorrect formulation or an impurity as a cause of the disorder.

The final atomic coordinates with their standard deviations and the final anisotropic and isotropic thermal parameters with their standard deviations are given in Tables III and IV. A table of observed and calculated structure factors is available.[27]

Polarographic Measurements. Voltammograms were obtained using a three-electrode multipurpose electrochemical instrument constructed from operational amplifiers.[28] The usual polarographic measurements were carried out using a rotating platinum electrode. All potentials were determined at 25 °C vs. a saturated calomel reference electrode. The working electrode consisted of a 0.13-mm diameter platinum wire sealed in a 5-mm o.d. glass tube. The 6-mm wire extended 3 mm downward from the bottom of the tube before making a 90° bend. Cyclic voltammetric current–potential curves obtained at scan rates of 0.05–0.1 V/s were recorded on an X-Y recorder, and those obtained at faster scans up to 225 V/s were displayed on a Tektronix oscilloscope. Solutions were ca. 1–2 mM in complex and 0.10 M in

Table III. Final Atomic Fractional Coordinates and Isotropic Thermal Parameters with Standard Deviations

Atom	*x*	*y*	*z*	*B*, Å^2
Ru(1)	0.0478 (1)	0.0467 (1)	0.2560^a	*b*
Ru(2)	0.0290 (1)	0.1778 (1)	0.2410 (3)	*b*
S(A1)	0.1764 (4)	0.0503 (4)	0.2088 (7)	*b*
S(A2)	0.0576 (5)	0.1084 (5)	0.1002 (8)	*b*
S(B1)	0.1505 (5)	0.2061 (4)	0.2995 (8)	*b*
S(B2)	0.0497 (5)	0.1191 (5)	0.3954 (9)	*b*
S(C1)	0.4228 (5)	0.4652 (4)	0.3014 (9)	*b*
S(C2)	0.4048 (5)	0.3380 (4)	0.1875 (9)	*b*
S(D1)	0.4850 (6)	0.2362 (5)	0.3526 (9)	*b*
S(D2)	0.0280 (5)	0.2749 (4)	0.1326 (10)	*b*
S(E1)	0.4647 (5)	0.4529 (5)	−0.3603 (9)	*b*
S(E2)	0.4348 (5)	0.4518 (5)	−0.1341 (8)	*b*
C(A)	0.1552 (17)	0.1008 (14)	0.0974 (26)	4.8 (7)
N(A)	0.1963 (19)	0.1358 (16)	0.0379 (23)	6.1 (8)
C(A1)	0.2788 (18)	0.1268 (15)	0.0484 (25)	5.6 (8)
C(A2)	0.3102 (19)	0.1803 (18)	0.1258 (30)	*b*
C(A3)	0.1670 (17)	0.1783 (15)	−0.0445 (26)	5.9 (8)
C(A4)	0.1558 (21)	0.1437 (17)	−0.1464 (32)	*b*
C(B)	0.1406 (22)	0.1484 (19)	0.4041 (34)	8.3 (10)
N(B)	0.1902 (17)	0.1348 (14)	0.4771 (22)	5.1 (7)
C(B1)	0.1743 (18)	0.0899 (15)	−0.4385 (27)	5.8 (8)
C(B2)	0.2158 (18)	0.0243 (15)	−0.4738 (25)	*b*
C(B3)	0.2607 (23)	0.1658 (19)	0.4721 (32)	8.8 (11)
C(B4)	0.2539 (30)	0.2236 (33)	0.5151 (47)	*b*
C(C)	0.3658 (15)	0.4044 (12)	0.2484 (35)	5.1 (6)
N(C)	0.2939 (12)	0.4040 (10)	0.2686 (22)	5.2 (6)
C(C1)	0.2613 (18)	0.4647 (16)	0.3223 (28)	7.2 (9)
C(C2)	0.2514 (26)	0.4520 (22)	0.4443 (34)	*b*
C(C3)	0.2485 (16)	0.3506 (14)	0.2437 (34)	6.3 (7)
C(C4)	0.2252 (18)	0.3586 (14)	0.1313 (38)	*b*
C(D)	0.0025 (17)	0.3167 (17)	0.2504 (41)	7.9 (9)
N(D)	0.0022 (16)	0.3838 (16)	0.2474 (45)	10.2 (8)
C(D1)	−0.0065 (31)	0.4088 (26)	0.3641 (52)	13.9 (18)
C(D2)	0.4265 (61)	0.0795 (46)	0.3519 (71)	*b*
C(D3)	0.0265 (27)	0.4203 (25)	0.1511 (50)	12.4 (17)
C(D4)	0.4657 (28)	0.0621 (26)	0.0871 (39)	*b*
C(E)	0.4461 (14)	0.4082 (11)	−0.2381 (32)	4.4 (6)
N(E)	0.4421 (13)	0.3416 (11)	−0.2568 (30)	6.7 (6)
C(E1)	0.4399 (24)	0.3008 (22)	−0.1448 (39)	9.5 (13)
C(E2)^c	0.3622 (22)	0.3059 (14)	−0.1333 (18)	*b*
C(E3)	0.4518 (21)	0.3068 (20)	−0.3470 (36)	7.1 (12)
C(E4)	0.0340 (26)	0.2259 (21)	−0.3666 (33)	*b*
B	0.3780 (–)^d	0.0960 (–)^d	−0.3000 (–)^d	15^d
F(1)^c	0.4268 (33)	0.1388 (17)	−0.2724 (77)	*b*
F(2)^c	0.3241 (21)	0.1242 (25)	−0.2527 (51)	*b*
F(3)^c	0.4080 (28)	0.0685 (13)	−0.1946 (26)	*b*
F(4)^c	0.3796 (29)	0.0683 (26)	−0.3608 (38)	*b*
X(1)^c	0.1212 (48)	0.3775 (33)	−0.1641 (63)	*b*
X(2)^c	0.1733 (34)	0.3378 (47)	−0.1903 (67)	*b*

^{a} Fractional coordinate fixed in order to define the origin in the *c* crystallographic direction. ^{b} Atoms refined anisotropically; see Table III. ^{c} Disordered atom; see text. ^{d} Atom positional and isotropic thermal parameters not refined (see text).

tetraethylammonium perchlorate as supporting electrolyte. Reagent grade DMF and acetonitrile were vacuum distilled from P_2O_5 and stored under a dry nitrogen atmosphere before use. Polarographic results are given in Table V.

Infrared spectra were recorded on a Perkin-Elmer Model 237 grating instrument. Electronic absorption spectra were obtained at 25 °C using a Cary Model 14 spectrophotometer. Nuclear magnetic resonance spectra were obtained on a Varian XL-100 instrument. A Yellow Springs Instrument Co. Model 31 conductivity bridge was used for the conductivity measurements. Molecular weight measurements were made using a Hewlett-Packard Model 302 vapor pressure osmometer. Chloroform solutions ca. 5×10^{-3} M in complex were used and measurements were made at 37 °C.

Results and Discussion

Synthesis and Characterization Data. The oxidation reaction of $M(R_2dtc)_3$ complexes which employs BF_3 gas under aerobic conditions has now been used by several research groups.[5,13,15,17] The reaction requires oxygen which presumably functions as the oxidizing agent. In the case where M = Ru(III) reaction 1 occurs. Other products of this reaction have not been characterized. Product Ia is firmly established for R = Me, Et, Bz, and pyrr and will be thoroughly discussed below. The presence of Ib was confirmed for R = Me and Et by infrared and ^1H NMR spectra[29] which match those of authentic samples synthesized according to Willemse.[30] An x-ray analysis[31] of the 3,5-bis(*N*,*N*-diethyliminium)-1,2,4-trithiolane dication, $[Et_4bitt]^{2+}$, showed the structure to be that represented by Ib. The tetraalkylthiuram disulfide, $(R_2dtc)_2$ (II), which is perhaps a more likely product of reaction 1, is rapidly oxidized to Ib by treatment with BF_3 gas in a stirred benzene solution open to the air. Hence it is likely that II is the initial product of reaction 1 and is oxidized to Ib by the oxidizing conditions employed.

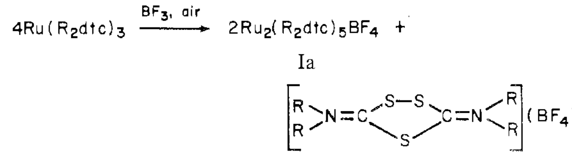

Ia
Ib
(1)

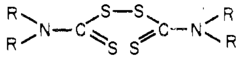
II

Analytical data and other characterization data for Ia are given in Tables I and VI. The molecular weight and conductivity results in $CHCl_3$ and CH_3NO_2 solutions, respectively, and the analytical data confirm the formula as $Ru_2(R_2dtc)_5BF_4$. The complexes are not significantly dissociated in $CHCl_3$ and behave as 1:1 electrolytes in CH_3NO_2. The complexes are diamagnetic in solid and solution phases.

Infrared spectra were measured in KBr disks. The data in the range 2000–700 cm^{-1} are given for R = Et in the Experimental Section and for the $S_2C{\overset{\dots}{-}}N$ stretch in Table I. The spectra are similar to the analogous $Ru(R_2dtc)_3$ complexes except that $\nu(C{\overset{\dots}{-}}N)$ is broadened and shifted to higher values in the oxidized products (Ia) (average shift for the four complexes 20 cm^{-1}) and BF_4^- has strong bands in the 1000–1100-cm^{-1} region. It is interesting to note that a similar increase in $\nu(C{\overset{\dots}{-}}N)$ has been observed on going from $Fe(R_2dtc)_3$ to its oxidized product $Fe(R_2dtc)_3BF_4$. In the latter case the increase results from the higher formal oxidation state of iron (+3 → +4) which causes an increased contribution of resonance structure IIIc. In the former case the formal oxidation state of Ru remains +3 but the positive charge on the $Ru_2(R_2dtc)_5^+$ cation causes a similar but smaller increased contribution of IIIc compared to $Ru(Et_2dtc)_3$; i.e., the positive charge is partially delocalized onto the ligands.

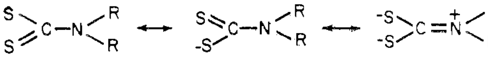
IIIa IIIb IIIc

Electronic spectra were measured in the range 30000–10000 cm^{-1} using DMF solutions and the maxima are given in Table VI. The spectra are rather nondistinct in this region consisting of three shoulders and a broad weak band at 10700 cm^{-1}. The corresponding $Ru(R_2dtc)_3$ complexes have much more intense bands in the same general regions (except for the one at 10700 cm^{-1} which is missing).

^1H NMR spectra were recorded in a number of solvents and are complex for all but R = Me due to spin–spin coupling and the low symmetry of the compounds. In the solid state the R = Et compound has no crystallographic symmetry (vide infra and Figure 1) but approximates C_2 symmetry especially if the methyl carbons are ignored. It is possible that the compounds have C_2 symmetry in solution which leaves three nonequivalent R_2dtc ligands. Since $S_2C{\overset{\dots}{-}}N$ bond rotation is likely to be slow on the ^1H NMR time scale at 30 °C, there should be five nonequivalent R groups. The ^1H NMR of the R = Me compound at 30 °C in CD_2Cl_2 solution shows five

Table IV. Anisotropic Thermal Parameters ($\times 10^4$)[a]

Atom	$10^4\beta_{11}$	$10^4\beta_{22}$	$10^4\beta_{33}$	$10^4\beta_{12}$	$10^4\beta_{13}$	$10^4\beta_{23}$
Ru(1)	35 (1)	24 (1)	93 (2)	0 (1)	−1 (2)	7 (2)
Ru(2)	37 (1)	26 (1)	94 (3)	−1 (1)	−5 (2)	7 (2)
S(A1)	31 (3)	31 (2)	86 (9)	3 (2)	−6 (4)	1 (4)
S(A2)	46 (5)	25 (3)	61 (9)	2 (3)	10 (5)	9 (4)
S(B1)	47 (4)	28 (3)	112 (10)	−11 (3)	−13 (5)	5 (4)
S(B2)	33 (4)	29 (3)	70 (9)	4 (3)	6 (5)	2 (4)
S(C1)	31 (3)	26 (3)	133 (11)	−1 (2)	6 (5)	−10 (4)
S(C2)	36 (4)	30 (3)	132 (11)	−5 (3)	−12 (5)	−12 (5)
S(D1)	71 (6)	41 (4)	105 (10)	−7 (4)	12 (7)	6 (5)
S(D2)	40 (4)	27 (3)	154 (12)	−3 (3)	−8 (6)	21 (5)
S(E1)	37 (4)	25 (3)	107 (9)	5 (3)	6 (5)	−2 (4)
S(E2)	49 (4)	28 (3)	61 (8)	−2 (3)	9 (5)	−1 (4)
C(S2)	54 (16)	44 (14)	124 (40)	2 (13)	−23 (22)	−14 (20)
C(A4)	61 (21)	37 (12)	159 (44)	−3 (13)	−27 (25)	−23 (19)
C(B2)	61 (17)	38 (12)	79 (3)	−2 (11)	−54 (19)	10 (14)
C(B4)	105 (31)	87 (39)	262 (78)	−22 (28)	−91 (41)	108 (44)
C(C2)	103 (24)	71 (18)	132 (41)	−33 (19)	−26 (27)	−56 (23)
C(C4)	45 (15)	28 (8)	299 (63)	−16 (9)	−8 (27)	−20 (20)
C(C2)	321 (88)	228 (67)	196 (119)	142 (63)	−79 (94)	25 (71)
C(D4)	79 (25)	101 (26)	200 (52)	39 (20)	−17 (32)	−46 (32)
C(E2)[c]	223 (28)	82 (12)	45 (19)	−15 (15)	38 (19)	102 (14)
C(E4)	127 (29)	65 (18)	93 (43)	34 (19)	−13 (32)	−9 (23)
F(1)[b]	223 (46)	65 (13)	1186 (206)	−69 (21)	140 (90)	28 (54)
F(2)[b]	119 (21)	176 (27)	338 (55)	42 (20)	62 (45)	33 (46)
F(3)[b]	245 (37)	81 (10)	243 (36)	18 (16)	−46 (29)	−11 (16)
F(4)[b]	265 (32)	144 (26)	259 (63)	−8 (23)	−105 (38)	−55 (32)
X(1)[b]	242 (71)	39 (31)	579 (102)	40 (35)	−321 (78)	−30 (44)
X(2)[b]	33 (31)	111 (67)	534 (132)	15 (37)	−41 (51)	88 (78)

[a] The form of the anisotropic thermal ellipsoid is $\exp[-(\beta_{11}h^2 + \ldots + 2\beta_{12}hk + \ldots)]$. [b] Disordered atom; see text. [c] Temperature factor is nonpositive definite; see text.

Table V. Polarographic Data for Dithiocarbamato Complexes of Ruthenium

Complex[b]	Process $z-1 \rightleftharpoons z$	$E_{1/2}$,[a] V; $\lvert E_{3/4}-E_{1/4}\rvert$, mV	
		Dimethylformamide	Acetonitrile
$Ru_2(Et_2dtc)_5{}^z$	$2+ \rightleftharpoons 1+$	c	+0.98; 85
	$1+ \rightleftharpoons 0$	−0.46; 57	−0.58; 58
	$0 \rightleftharpoons 1-$	−1.05; 95	−1.11; 74
$Ru(Et_2dtc)_3{}^z$	$1+ \rightleftharpoons 0$	+0.38; 70	
	$0 \rightleftharpoons 1-$	−0.75; 60	
$Ru_2(Me_2dtc)_5{}^z$	$2+ \rightleftharpoons 1+$	c	+1.03; 74
	$1+ \rightleftharpoons 0$	−0.45; 55	−0.52; 59
	$0 \rightleftharpoons 1-$	−0.96; 65	−1.00; 73
$Ru(Me_2dtc)_3{}^z$	$1+ \rightleftharpoons 0$	+0.48; 69	
	$0 \rightleftharpoons 1-$	−0.72; 59	
$Ru_2(Bz_2dtc)_5{}^z$	$2+ \rightleftharpoons 1+$	c	+1.04; c
	$1+ \rightleftharpoons 0$	−0.31	−0.40; 58
	$0 \rightleftharpoons 1-$	c	−0.93; 100
$Ru(Bz_2dtc)_3{}^z$	$1+ \rightleftharpoons 0$	+0.51; 86	
	$0 \rightleftharpoons 1-$	−0.59; 65	
$Ru_2(pyrr(dtc))_5{}^z$	$2+ \rightleftharpoons 1+$	c	+0.99; c
	$1+ \rightleftharpoons 0$	−0.44; 61	−0.53; 53
	$0 \rightleftharpoons 1-$		−1.02; 63
$Ru(pyrr(dtc))_3{}^z$	$1+ \rightleftharpoons 0$	+0.40; 69	
	$0 \rightleftharpoons 1-$	−0.74; 66	

[a] All potentials were determined at 25 °C vs. SCE using a rotating platinum electrode. [b] Data obtained from solutions prepared from $z = 1+$ and 0 species for $Ru_2(dtc)_5{}^z$ and $Ru(dtc)_3{}^z$, respectively. [c] Polarographic waves not well developed.

Table VI. Electronic Spectral Data for $[Ru_2(R_2dtc)_5]BF_4$ Complexes in DMF Solution

R	λ_{max} (ϵ)[a]
C_2H_5[b]	~25 000 sh (4580), ~21 100 sh (2180), ~18 000 sh (778), 10 700 (173)
CH_3	~25 000 sh (4270), ~21 600 sh (2090), ~18 200 sh (644), 10 700 (155)
$CH_2C_6H_5$	~22 200 sh (3740), ~18 200 sh (1250), ~11 800 sh (174)
$(CH_2)_4$	~25 000 sh (3470), ~22 400 sh (2180), ~18 200 sh (600), 10 700 (150)

[a] cm^{-1} (M^{-1} cm^{-1}); apparent ϵ values, uncorrected for underlying absorption. [b] Comparison data for $Ru(Et_2dtc)_3$: 27 300 (10 300), 21 200 (2920), 17 700 (1780).

singlets of equal intensity at 3.046, 3.144, 3.430, 3.468, and 3.500 ppm downfield from TMS. An alternate explanation exists in which case the complex has no symmetry and S_2C N bond rotation is fast on the ^1H NMR time scale. Lowering of the temperature to −90 °C does not result in further splitting of the Me resonances so the former explanation is the most reasonable. ^1H NMR spectra of the R = Me complex were recorded at temperatures up to 70 °C using a variety of solvents with no signs of coalescence. This observation indicates that $S_2C\overset{\cdots}{-}N$ bond rotation must still be slow on the ^1H NMR time scale at 70 °C.

Polarographic Study. Polarographic data were obtained for $Ru(R_2dtc)_3$ and $[Ru_2(R_2dtc)_5]BF_4$ complexes and are given in Table V. The latter complexes are electroactive and voltammetric results indicate the existence of a four-membered series (IV) in acetonitrile. The one-electron nature of these

$$[Ru_2(R_2dtc)_5]^{2+} \rightleftarrows [Ru_2(R_2dtc)_5]^{+} \rightleftarrows$$
$$[Ru_2(R_2dtc)_5]^{0} \rightleftarrows [Ru_2(R_2dtc)_5]^{-}$$

IV

processes has been established for R = Et by comparison of diffusion currents with those of known one-electron processes of $M(Et_2dtc)_3$ where R = Fe and Ru[6,18] and by isolation of $[Ru_2(Et_2dtc)_5]^0$.[32] Judging from the reversibility criterion $|E_{3/4} - E_{1/4}| = 59$ mV, only the $1+ \rightleftharpoons 0$ process is reversible. This is confirmed by cyclic voltammetry for $1+ \rightleftharpoons 0$ where $i_{p,a}/i_{p,c} = 1.00$ and $\Delta E_p = 53$ mV for R = Et in DMF. The other processes are irreversible and no attempts have been made to isolate the 2+ or 1− species. The neutral species, however, is easily synthesized by reduction of the 1+ complex with $NaBH_4$. This new purple complex presumably maintains the $Ru_2(R_2dtc)_5$ stoichiometry in solution because it can be air oxidized back to the 1+ complex and its polarographic half-wave potentials are identical with those of $[Ru_2dtc_5]^+$. Attempts to synthesize the neutral complex by controlled-potential electrolysis in DMF and CH_3CN have not been successful. Details of this work will be the subject of another paper.[33]

The half-wave potentials for dithiocarbamatometal com-

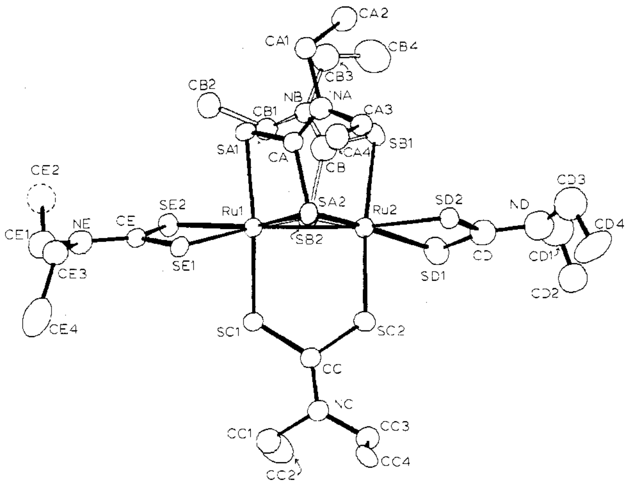

Figure 1. Drawing of the $[Ru_2(Et_2dtc)_5]^+$ ion viewed along the crystallographic *c* axis; definition of numbering system.

plexes are known to display a consistent dependence upon the N substituent.[6,34-36] In previous work[6,36] the order for ease of oxidation is Bz << pyrr < Me < Et with Bz being hardest to oxidize (i.e., more positive potential). This trend which is independent of metal is generally confirmed with $Ru(R_2dtc)_3$ and $[Ru_2(R_2dtc)_5]^+$ complexes, except that the order of pyrr and Me is usually reversed.

The polarographic results for $Ru(R_2dtc)_3$ complexes (Table V) reveal a three-membered series (V) which is in agreement

$$[Ru(R_2dtc)_3]^+ \rightleftarrows [Ru(R_2dtc)_3]^0 \rightleftarrows [Ru(R_2dtc)_3]^-$$

V

with a previous study.[18] Only the central member of this series has been isolated to date. The 0 ⇄ 1− process is reversible by cyclic voltammetry ($i_{p,a}/i_{p,c} = 0.97$ and $\Delta E_p = 59$ mV) whereas the 0 ⇌ 1+ process is irreversible ($i_{p,a}/i_{p,c} = 1.6$ and $\Delta E_p = 98$ mV). Comparison of these results to those of the corresponding iron complexes is interesting. Voltammetry of $Fe(Et_2dtc)_3$ in DMF reveals a one-electron reduction at −0.447 V and a reversible one-electron oxidation at a potential (+0.423 V) only slightly different from that of its ruthenium analogue.[18] The similarity of these potentials for the 0 ⇌ 1+ process and the isolation of $[Fe(Et_2dtc)_3]^+$ [5-10] suggest that $[Ru(Et_2dtc)_3]^+$ should be synthetically accessible. However, in the case of ruthenium the process is irreversible even for cyclic voltammetric scan speeds as fast as 225 V/s. All attempts to prepare $[Ru(R_2dtc)_3]^+$ have failed including controlled-potential electrolysis. It is not clear why chemical oxidation of $Ru(R_2dtc)_3$ with BF_3–air yields $[Ru_2(R_2dtc)_5]^+$ whereas the analogous oxidation reaction with $Fe(R_2dtc)_3$ yields $[Fe(R_2dtc)_3]^+$. Perhaps the increased tendency toward metal–metal bonding for ruthenium provides the driving force for this reaction.[37] $[Ru_2(Et_2dtc)_5]^+$ has a short Ru–Ru bond (vide infra). It is interesting to note that oxidation of $Ru(R_2dtc)_3$ with I_2 yields a gold diamagnetic product[32] which is not $[Ru_2(R_2dtc)_5]^+$ whereas in the case of iron the product contains paramagnetic $[Fe(R_2dtc)_3]^+$.[38] Electrochemical oxidation of $Ru(Et_2dtc)_3$ yields yet another diamagnetic complex. These various oxidation reactions are under current investigation.

Structural Study. General Description of the Structure. The crystal structure was determined for $[Ru_2(Et_2dtc)_5]BF_4 \cdot C_3H_6O$. The crystal data are given in Table II. The structure of the cationic unit and the numbering system used throughout this paper are shown in Figure 1. The ORTEP stereoview shown in Figure 2 more clearly illustrates the spatial geometry of the ligands and Figure 3 shows the $Ru_2S_{10}C_5$ core minus ligand C in a view which has been rotated ~90° about the Ru–Ru bond such that ligand C points into the paper. The structural results are novel because this is the first example where dithiocarbamate ligands connect two metals in both bridging fashions simultaneously. Each ruthenium atom is seven-coordinate if the metal–metal bond is counted. The diamagnetism of the compound results from spin pairing via the Ru–Ru bond (2.743 Å) of two low-spin Ru(III) d^5 ions. Distortions from idealized octahedral symmetry at each ruthenium atom result in part from metal–metal bonding and partly from the geometrical constraints of the four-membered dithiocarbamate chelate rings.

The ability of dithiocarbamate ligands to bridge two metal atoms as found for ligand C probably requires a short metal–metal bond. This mode of bonding which is similar to that of simple carboxylate anions in a number of transition metal complexes[39] is now well established for thioxanthate[40] (Va)

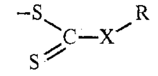

R = alkyl
Va, X = S
b, X = O

and xanthate[41] (Vb) ligands. In these cases short metal–metal bonds are found. In a copper tetramer the dithiocarbamate ligand is also known to bridge two metal atoms in this fashion.[42]

The other bridging mode which is illustrated by ligands A and B has not previously been observed for dithiocarbamate ligands. Several examples[43] of dimeric bis-chelate complexes of zinc and copper with monobridging dithiocarbamate ligands are known but in these cases the M–S–M' bridge is not symmetric whereas in the present ruthenium structure, the Ru–S and Ru'–S distances are the same within experimental error.

Ru_2S_{10} Core. Interatomic distances and angles within the Ru_2S_{10} core are given in Table VII. The Ru–Ru bond length is short (2.743 (3) Å compared to 2.650 Å found in elemental ruthenium[44]) but not nearly as short as 2.281 Å found in $Ru_2(O_2CC_3H_7)_4Cl$ which consists of ruthenium ions in the $+2^1/_2$ oxidation state.[45] These distances may be compared with 2.848 Å found in $Ru_3(CO)_{12}$[46] and the range 2.70–2.95 Å observed in a number of ruthenium carbonyl cluster

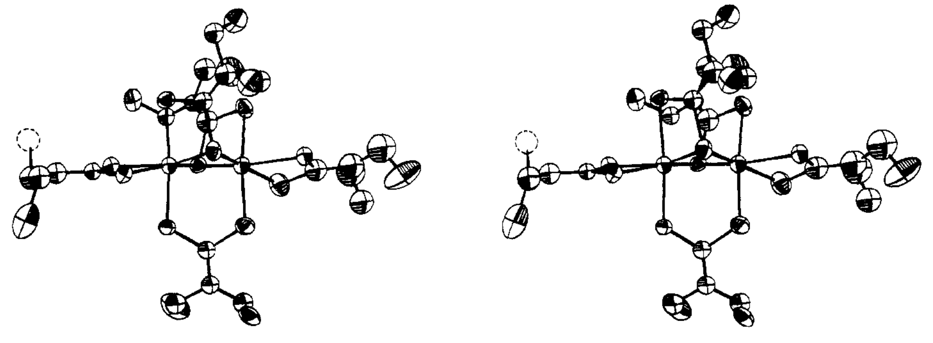

Figure 2. ORTEP stereoview showing the thermal ellipsoids. Ellipsoids are 25% probability surfaces.

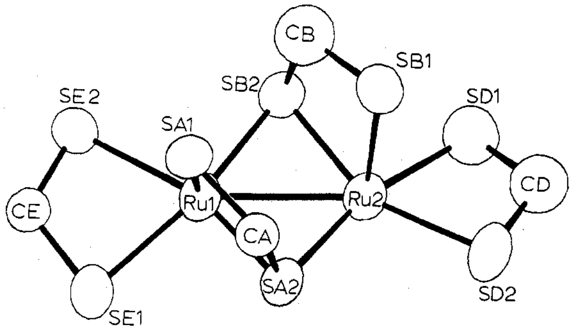

Figure 3. Drawing of the $Ru_2S_{10}C_5$ core in a view approximately along the *a* crystallographic axis. Ligand C has been omitted for clarity.

Table VII. Interatomic Distances and Angles in the Ru_2S_{10} Core[a]

	Distances, Å		
Ru(1)–Ru(2)	2.743 (3)		
Ru(1)–S(A1)	2.428 (8)	Ru(2)–S(B1)	2.412 (9)
Ru(1)–S(A2)	2.325 (10)	Ru(2)–S(B2)	2.300 (11)
Ru(1)–S(B2)	2.290 (11)	Ru(2)–S(A2)	2.324 (11)
Ru(1)–S(C1)	2.369 (9)	Ru(2)–S(C2)	2.391 (9)
Ru(1)–S(E1)	2.433 (11)	Ru(2)–S(D1)	2.395 (11)
Ru(1)–S(E2)	2.414 (11)	Ru(2)–S(D2)	2.422 (11)
S(A1)–S(A2)	2.828 (13)	S(B1)–S(B2)	2.839 (13)
S(E1)–S(E2)	2.861 (15)	S(D1)–S(D2)	2.852 (16)
S(C1)–S(C2)	3.009 (13)	S(A2)–S(B2)	3.675 (15)
	Angles, Deg		
Ru(1)–S(A2)–Ru(2)	72.3 (3)	Ru(1)–S(B2)–Ru(2)	73.4 (3)
S(A1)–Ru(1)–S(A2)	73.0 (3)	S(B1)–Ru(2)–S(B2)	74.0 (3)
S(E1)–Ru(1)–S(E2)	72.4 (4)	S(D1)–Ru(2)–S(D2)	72.7 (4)
Ru(1)–Ru(2)–S(C2)	90.2 (2)	Ru(2)–Ru(1)–S(C1)	89.9 (2)
S(A2)–Ru(1)–S(B2)	105.6 (4)	S(A2)–Ru(2)–S(B2)	105.3 (4)
S(C1)–Ru(1)–S(E1)	88.1 (3)	S(C2)–Ru(2)–S(D1)	86.7 (4)
S(A1)–Ru(1)–S(E2)	91.9 (3)	S(B1)–Ru(2)–S(D2)	88.4 (3)
S(A1)–Ru(1)–S(C1)	175.8 (3)	S(B1)–Ru(2)–S(C2)	173.6 (3)
S(A2)–Ru(1)–S(E2)	155.1 (4)	S(A2)–Ru(2)–S(D1)	166.1 (4)
S(B2)–Ru(1)–S(E1)	166.8 (4)	S(B2)–Ru(2)–S(D2)	154.6 (4)

[a] For numbering system see Figure 1.

compounds.[47] A discussion of the bonding scheme will be presented in a later section.

Four types of Ru–S bonds can be identified in the structure. The average Ru–S bond lengths for these types are 2.416 Å for terminal chelated ligands D and E, 2.420 Å to nonbridging sulfur atoms of monobridging ligands A and B, 2.310 Å to bridging sulfur atoms of monobridging ligands A and B, and 2.380 Å for the dibridging ligand C. Within each type all distances are within 2σ of the mean. These distances can be compared to 2.376 Å which is the average value found in $Ru(Et_2dtc)_3$.[48] The Ru–S distances to bridging sulfur atoms S(A2) and S(B2) are significantly shorter than the others while the terminal distances are longer than those found in $Ru(Et_2dtc)_3$. Since the latter bonds are trans to the former, a trans effect may be operative. The distances to sulfur atoms of the dibridging ligand are ~2% shorter than the terminal distances. This trend has been noted in other bidentate-chelate complexes where both four- and five-membered chelate rings with one or more metal atoms are present.[40,49]

All of the four-membered chelate rings have essentially the same bite angle size (average 73.0° with a standard deviation from the mean of 0.7 Å) which is identical with that found in $Ru(Et_2dtc)_3$.[48] The "bite" angles in ligand C, S(C1)–Ru(1)–Ru(2) and S(C2)–Ru(2)–Ru(1), are 90.2 (2) and 89.9 (2)°, respectively. The average of the four S–S bite distances for the four-membered chelate rings is 2.845 Å with a standard deviation from the mean of 0.015 Å, while the bite distance for the five-membered chelate ring is 3.009 (13) Å. This trend is also found in bis(ethyl thioxanthato)-μ-bis(ethyl thioxanthato)-μ-bis(ethylthio)-diiron(III) (VI)[40] and is expected for compounds which contain both four- and five-membered chelate rings.[40,50] Compound VI is interesting in that the Fe_2S_{10} core is very similar to the Ru_2S_{10} core of [$Ru_2(Et_2dtc)_5$]$^+$. The Fe(III)–Fe(III) distance in VI is 2.618 Å.

Table VIII. Weighted Least-Squares Planes and the Distances of the Atoms from Their Respective Planes[a]

Plane	Atoms and distances from planes, Å
1	Ru(1), −0.08 (1); Ru(2), −0.08 (1); S(A2), 0.20 (1); S(B2), 0.21 (1)
2	S(A1), 0.02 (3); S(A2), 0.01 (3); C(A), −0.08 (4); N(A), 0.02 (4); C(A1), 0.00 (5); C(A3), 0.01 (5); Ru(1), 0.28 (4)[b]
3	Ru(2), −0.02 (3); S(B1), 0.06 (4); S(B2), 0.05 (4); C(B), −0.02 (4); N(B), −0.02 (4); C(B1), −0.00 (5); C(B3), −0.02 (5)
4	S(C1), −0.07 (3); S(C2), 0.03 (3); C(C), 0.07 (4); N(C), 0.02 (4); C(C1), 0.06 (5); C(C3), −0.01 (3); Ru(1), 0.03 (4);[b] Ru(2), −0.99 (4)[b]
5	S(D1), −0.01 (5); S(D2), 0.05 (5); C(D), −0.05 (5); N(D), −0.10 (5); C(D1), 0.10 (7); C(D3), 0.01 (7); Ru(2), 0.46 (4)[b]
6	Ru(1), 0.00 (3); S(E1), 0.07 (4); S(E2), −0.05 (4); C(E), −0.01 (5); N(E), −0.07 (5); C(E1), 0.12 (6);[c] C(E3), −0.05 (6)

	Parameters from Equation of Planes of the Form $AX + BY + CZ - D = 0$			
Plane	*A*	*B*	*C*	*D*
1	0.9873	0.1443	0.0218	−0.0636
2	0.9770	0.0813	0.1798	−0.0811
3	−0.3414	0.8260	0.3845	−0.2308
4	−0.1536	−0.6236	−0.7325	0.2258
5	0.9835	−0.0294	0.1741	−0.0395
6	−0.9938	−0.0352	0.1034	0.0227

[a] For numbering system see Figure 1. [b] Atom not included in the calculation of the plane. [c] Bonded to a disordered atom.

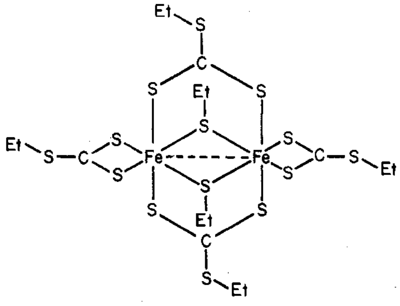

VI

The four-membered ring formed by Ru(1), S(A2), Ru(2), and S(B2) is not planar as evidenced by plane 1 in Table VIII and has interior angles which are nearly identical with those found in the $Fe_2(SEt)_2$ ring of compound VI: Ru(1)–S(A2)–Ru(2) = 72.3 (3)°, Ru(1)–S(B2)–Ru(2) = 73.4 (3)°, S(A2)–Ru(1)–S(B2) = 105.6 (4)°, and S(A2)–Ru(2)–S(B2) = 105.3 (4)°, compared to Fe–S–Fe = 72.4 (1)° and S–Fe–S = 107.7 (1)° in IV.[40]

Geometry of the Ligands. The interatomic distances and angles for the five ligands A–E are given in Table IX. The average of the ten C$\overset{\dots}{-}$S bond lengths is 1.75 Å with a standard deviation from the mean of 0.06 Å. This value is slightly larger but similar to the average C$\overset{\dots}{-}$S bond distance obtained in $Ru(Et_2dtc)_3$ (1.72 Å)[48] and other related compounds.[8] The average of the five $S_2C\overset{\dots}{-}N$ bond lengths is 1.34 Å with a standard deviation from the mean of 0.05 Å. This value is similar to distances observed in related compounds[8,48] and indicates significant contribution from resonance structure (IIIc). The remaining ligand distances are similar to values observed in related compounds.[4,48] The values of the angles in the four-membered chelating ligands are similar to values observed in $Ru(Et_2dtc)_3$[48] and values found within the five-membered chelate ring are similar to values observed in

Table IX. Interatomic Distances and Angles in the Ligands[a]

	Ligand A	Ligand B	Ligand C	Ligand D	Ligand E
			Distances, Å		
S(1)–C	1.78 (3)	1.77 (4)	1.76 (2)	1.71 (5)	1.81 (4)
S(2)–C	1.79 (3)	1.77 (4)	1.72 (2)	1.76 (5)	1.59 (3)
C–N	1.28 (4)	1.31 (5)	1.34 (4)	1.39 (5)	1.40 (5)
N–C(1)	1.53 (5)	1.43 (4)	1.54 (5)	1.55 (7)	1.63 (6)
N–C(3)	1.45 (4)	1.44 (5)	1.42 (3)	1.48 (8)	1.34 (6)
C(1)–C(2)	1.58 (5)	1.62 (4)	1.55 (6)	1.26 (12)	1.43 (6)
C(3)–C(4)	1.47 (5)	1.31 (8)	1.47 (6)	1.42 (7)	1.67 (6)
			Angles, Deg		
Ru(1)–S(1)–C	90 (1)		114 (1)		84 (1)
Ru(1)–S(2)–C	93 (1)	106 (1)			89 (1)
Ru(2)–S(1)–C		88 (1)		89 (1)	
Ru(2)–S(2)–C	107 (1)	91 (1)	112 (1)	87 (1)	
S(1)–C–S(2)	105 (2)	106 (2)	119 (1)	111 (2)	115 (1)
S(1)–C–N	131 (3)	125 (3)	121 (2)	131 (4)	112 (3)
S(2)–C–N	123 (3)	128 (3)	119 (2)	118 (4)	133 (3)
C–N–C(1)	118 (3)	120 (3)	117 (3)	108 (4)	112 (4)
C–N–C(3)	122 (3)	120 (3)	123 (3)	122 (5)	131 (4)
N–C(1)–C(2)	109 (3)	105 (3)	109 (3)	93 (6)	94 (3)
N–C(3)–C(4)	111 (3)	108 (4)	107 (3)	110 (4)	117 (3)

[a] For numbering system, see Figure 1.

the analogous rings of compound VI.[40] The angles and distances associated with the methyl carbon atoms have large errors (especially ligand D) due to disorder in the BF_4 counterion and the acetone of solvation.

Weighted least-squares planes for the five ligands and the distances of the atoms from the planes are given in Table VIII. All of the S_2CNC_2 groupings are planar within experimental error. For ligands B and E the planes include the ruthenium atom whereas the metal atoms are not in the plane for ligands A and D. In ligand C, the five-membered chelate ring ligand, only one of the two ruthenium atoms is not in the plane formed by S_2CNC_2.

Intermolecular Distances. There are no abnormally short intermolecular contacts; however, one short intramolecular nonbonded carbon–carbon distance is observed. The methyl–methyl distance between C(D2) and C(D4) is 3.38 (10) Å which is less than 3.60 Å, the sum of the van der Waals radii for carbon. This distance is not uncommonly short for methyl–methyl distances, however.[51] The shortest distance between the BF_4 anion and the cation is 3.38 (6) Å for F(2)–C(A4) and between the acetone molecule and the cation is 3.59 Å for X(2)–C(E2).

Metal–Metal Bonding. The observed ruthenium–ruthenium bond length of 2.743 Å is within the range (2.28–2.95 Å) of crystallographically determined values for which metal–metal bonding has been postulated.[45-47] Two additional features suggest the presence of a ruthenium–ruthenium bond. In other complexes which contain M_2X_2 rings, where X is the donor atom of a bridging ligand, "sharply acute" M–X–M angles are characteristic of metal–metal bonding.[52] In $[Ru_2(Et_2dtc)_5]^+$, the Ru(1)–S(A2)–Ru(2) and Ru(1)–S(B2)–Ru(2) angles are 72.3 and 73.4°, respectively. Another fact which is taken as evidence[53] for a ruthenium–ruthenium bond is that the ruthenium–ruthenium bond length is significantly shorter than the bite distance of ligand C, 3.009 (13) Å.

The diamagnetism of the compound can also be used as evidence for metal–metal bonding because each ruthenium(III) atom is low-spin d^5 and a single bond involving overlap of two T_{2g} metal orbitals (assuming idealized O_h geometry) will account for the diamagnetism. Of course spin pairing via the bridging sulfur atoms can also account for the diamagnetism. The ruthenium–ruthenium bonding can be described in terms of a qualitative molecular orbital scheme involving direct overlap of ruthenium d orbitals. This scheme has been thoroughly described elsewhere.[40]

Acknowledgment. This research was supported by Grant GP-37795 from the National Science Foundation, by the Research Corp., and by the University of Minnesota Computer Center. The assistance of Professor D. Britton is also gratefully acknowledged.

Registry No. $[Ru_2(Me_2dtc)_5]BF_4$, 57774-53-5; $[Ru_2(Et_2dtc)_5]BF_4\cdot C_3H_6O$, 55326-22-2; $[Ru_2(Bz_2dtc)_5]BF_4$, 57774-55-7; $[Ru_2(pyrr(dtc))_5]BF_4$, 57774-57-9; $Ru(Et_2dtc)_3$, 31656-15-2; $Ru(Me_2dtc)_3$, 43190-67-6; $Ru(Bz_2dtc)_3$, 51751-58-7; $Ru(pyrr(dtc))_3$, 57527-43-2; BF_3, 7637-07-2.

Supplementary Material Available: listing of structure factor amplitudes (12 pages). Ordering information is given on any current masthead page.

References and Notes

(1) H. C. Brinkhoff, *Recl. Trav. Chim. Pays-Bas*, **90**, 377 (1971); H. C. Brinkhoff, Ph.D. Thesis, Nijmegen, 1970.
(2) J. P. Fackler, Jr., A. Avdeef, and R. G. Fischer, Jr., *J. Am. Chem. Soc.*, **95**, 744 (1973).
(3) P. T. Beurskens and J. A. Cras, *J. Cryst. Mol. Struct.*, **1**, 63 (1971).
(4) J. Willemse, Ph.D. Thesis, Nijmegen, 1974.
(5) E. A. Pasek and D. K. Straub, *Inorg. Chem.*, **11**, 259 (1972).
(6) R. Chant, A. R. Hendrickson, R. L. Martin, and N. M. Rohde, *Aust. J. Chem.*, **26**, 2533 (1973).
(7) R. M. Golding, C. M. Harris, K. J. Jessop, and W. C. Tennant, *Aust. J. Chem.*, **25**, 2567 (1972).
(8) R. L. Martin, N. M. Rohde, G. B. Robertson, and D. Taylor, *J. Am. Chem. Soc.*, **96**, 3647 (1974).
(9) M. C. Palazzotto, D. J. Duffy, B. L. Edgar, L. Que, Jr., and L. H. Pignolet, *J. Am. Chem. Soc.*, **95**, 4537 (1973).
(10) M. C. Palazzotto and L. H. Pignolet, *Inorg. Chem.*, **13**, 1781 (1974).
(11) K. L. Brown, *Cryst. Struct. Commun.*, **3**, 493 (1974).
(12) K. L. Brown, R. M. Golding, P. C. Healy, K. J. Jessop, and W. C. Tennant, *Aust. J. Chem.*, **27**, 2075 (1974).
(13) R. Y. Saleh and D. K. Straub, *Inorg. Chem.*, **13**, 3017 (1974).
(14) J. Willemse and J. A. Cras, *Recl. Trav. Chim. Pays-Bas*, **91**, 1309 (1972).
(15) L. R. Gahan and M. J. O'Connor, *J. Chem. Soc., Chem. Commun.*, 67 (1974).
(16) The preparation of this compound is similar to the one leading to a diamagnetic product; however, the yield of the paramagnetic product is low and is obtained as a brown residue after extensive washing with benzene. Our observations suggest that the brown paramagnetic Co(IV) complex is a minor product of the BF_3 air oxidation of impure $Co(R_2dtc)_3$ and cannot be isolated at all if the $Co(R_2dtc)_3$ is carefully chromatographed to remove a brown impurity.
(17) A. R. Hendrickson and R. L. Martin, *J. Chem. Soc., Chem. Commun.*, 873 (1974).
(18) G. S. Patterson and R. H. Holm, *Inorg. Chem.*, **11**, 2285 (1972).
(19) Abbreviations used throughout for N substituents: Me = CH_3, Et = C_2H_5, Bz = $CH_2C_6H_5$, pyrr = $(CH_2)_4$.
(20) L. H. Pignolet and B. M. Mattson, *J. Chem. Soc., Chem. Commun.*, 49 (1975).
(21) D. J. Duffy and L. H. Pignolet, *Inorg. Chem.*, **13**, 2045 (1974).
(22) P. W. R. Corfield, R. J. Doedens, and J. A. Ibers, *Inorg. Chem.*, **6**, 197 (1967).
(23) P. Coppens, L. Leiserowitz, and D. Rabinovich, *Acta Crystallogr.*, **18**, 1035 (1965).
(24) Two local programs by Dr. L. W. Finger were used: UMPREL for statistics and Patterson map and BADTEA for bond distances, angles, and errors. Full-matrix least-squares refinement and Fourier maps were performed with the following computer programs, respectively: LINUS51, a local version of LINUS, the Busing–Levy Fortran least-squares program as modified by Hamilton and Ibers, and JIMDAP, a local version of Zalkin's Fourier program FORDAP, as modified by Ibers. The last two programs were kindly provided by Dr. V. R. Magnuson. All data processing was done with the CDC CYBER74 computer at the University of Minneapolis Computer Center.
(25) $R_1 = \sum||F_o| - |F_c||/\sum|F_o|$ and $R_2 = (\sum w(|F_o| - |F_c|)^2/\sum wF_o^2)^{1/2}$; the numerator of R_2 was the function minimized where $|F_o|$ and $|F_c|$ are the observed and calculated structure amplitudes and where the weights, w, are taken as $4F_o^2/\sigma^2(F_o^2)$. Atomic scattering factors were taken from the "International Tables for X-Ray Crystallography", Vol. III, Kynoch Press, Birmingham, England, 1962, Table 3.3.1A (S, C, N, B, F) and Table 3.3.1B (Ru). Anomalous dispersion corrections from the same source (Table 3.3.2C) were used for ruthenium: $\Delta f' = -1.2$, $\Delta f'' = 1.1$.
(26) One of the methyl carbon atoms, C(E2), had a nonpositive definite temperature factor.
(27) Supplementary material.
(28) R. B. Fulton, Ph.D. Thesis, University of Minnesota, Minneapolis, Minn., 1968.
(29) Spectral results for $[R_4bitt]^{2+}$, R = Et: ir (KBr disk) ν(C–N) 1557 cm^{-1}; ^1H NMR (in CD_3CN) multiplet of six peaks which are believed to be two quartets centered at 1.12 ppm upfield from CHD_2CN and a triplet at 0.73 ppm downfield from CHD_2CN.
(30) J. Willemse and J. J. Steggerda, *Chem. Commun.*, 1123 (1969).
(31) P. T. Beurskens, W. P. J. H. Bosman, and J. A. Cras, *J. Cryst. Mol. Struct.*, **2**, 183 (1972).
(32) B. M. Mattson, work in progress.

(33) B. M. Mattson, J. R. Heiman, and L. H. Pignolet, to be submitted for publication.
(34) A. M. Bond, A. R. Hendrickson, and R. L. Martin, *J. Am. Chem. Soc.*, **95**, 1449 (1973).
(35) L. H. Pignolet, G. S. Patterson, J. F. Weiher, and R. H. Holm, *Inorg. Chem.*, **13**, 1263 (1974).
(36) A. R. Hendrickson, R. L. Martin, and N. M. Rohde, *Inorg. Chem.*, **13**, 1933 (1974).
(37) F. A. Cotton, *Acc. Chem. Res.*, **2**, 240 (1969).
(38) The $[Fe(Me_2dtc)_3]^+$ cation has been characterized by electronic absorption, ^1H NMR, and ir spectroscopy.
(39) C. Oldham, *Prog. Inorg. Chem.*, **10**, 223 (1968).
(40) D. Coucouvanis, S. J. Lippard, and J. A. Zubieta, *Inorg. Chem.*, **9**, 2775 (1970).
(41) L. Ricard, P. Karagiannidis, and R. Weiss, *Inorg. Chem.*, **12**, 2179 (1973).
(42) R. Hesse, *Ark. Kemi*, **20**, 481 (1963).
(43) M. Monamico, G. Dessy, A. Mugnoli, A. Vaciago, and L. Zambonelli, *Acta Crystallogr.*, **19**, 885, 889 (1965).
(44) H. Hellawell and W. Hume-Rothery, *Philos. Mag.*, **45**, 797 (1954).
(45) M. J. Bennett, K. G. Caulton, and F. A. Cotton, *Inorg. Chem.*, **8** (1969); F. A. Cotton, *Chem. Soc. Rev.*, **4**, 27 (1975).
(46) R. Mason and A. I. M. Rae, *J. Chem. Soc. A*, 778 (1968).
(47) (a) R. Belford, M. I. Bruce, M. A. Cairns, M. Green, H. P. Taylor, and P. Woodward, *Chem. Commun.*, 1159 (1970); (b) M. R. Churchill, K. Gold, and P. H. Bird, *Inorg. Chem.*, **8**, 1956 (1969); (c) M. R. Churchill and J. Wormald, *J. Am. Chem. Soc.*, **93**, 5670 (1971); (d) R. Mason and W. R. Robinson, *Chem. Commun.*, 468 (1968); (e) P. J. Roberts and J. Trotter, *J. Chem. Soc. A*, 3246 (1970); (f) D. B. W. Yawney and R. J. Doedens, *Inorg. Chem.*, **11**, 838 (1972); (g) M. R. Churchill and J. Wormald, *ibid.*, **12**, 191 (1973).
(48) L. H. Pignolet, *Inorg. Chem.*, **13**, 2051 (1974).
(49) D. Coucouvanis and S. J. Lippard, *J. Am. Chem. Soc.*, **91**, 307 (1969).
(50) R. Eisenberg, *Prog. Inorg. Chem.*, **12**, 295 (1970).
(51) H. Abrahamson, J. R. Heiman, and L. H. Pignolet, *Inorg. Chem.*, **14**, 2070 (1975), and references cited therein.
(52) L. F. Dahl, E. R. de Gil, and R. D. Feltham, *J. Am. Chem. Soc.*, **91**, 1653 (1969).
(53) F. A. Cotton, *Rev. Pure Appl. Chem.*, **17**, 25 (1967).

Contribution from the Department of Chemistry,
University of Alberta, Edmonton, Alberta, Canada T6G 2E1

Bis(dimethyldithioarsinato)oxovanadium(IV) and Its Complexes with Lewis Bases

E. D. DAY and R. E. D. McCLUNG*

Received September 3, 1975 AIC506553

The preparation and physical characteristics of bis(dimethyldithioarsinato)oxovanadium(IV) and the results of an ESR investigation of the interaction of this complex with Lewis bases in toluene solutions are described. Thermogravimetric, infrared, mass spectral, and magnetic susceptibility data for the complex are given, as well as thermogravimetric and infrared data for a green solid, $OV[S_2As(CH_3)_2]_2 \cdot x py$ with $x \simeq 4$, obtained by solvent removal from a pyridine solution of the complex. The ESR results indicate that the behavior of the dithioarsinate complex with Lewis bases is similar to that of the corresponding dithiophosphinate complex in that the chelating ligands sequentially become monodentate with a Lewis base molecule occupying the coordination site from which the sulfur atom is displaced. The equilibrium constants and thermodynamic parameters for the ligand displacement equilibria are reported.

Introduction

In a previous electron spin resonance (ESR) study in this laboratory,[1] which was substantiated independently,[2,3] the coordination of Lewis bases to vanadyl dithiophosphinate complexes was illucidated. On the basis of ESR, optical, and infrared measurements on the complexes $OV(S_2PX_2)_2$, X = CH_3,[1] C_6H_5,[1] and OC_2H_5,[1-3] in solutions containing various concentrations of the Lewis bases pyridine,[1-3] hexamethylphosphoramide,[1] or dimethylformamide,[1] it was concluded that the equilibria 1 and 2, where Y is phosphorus and L is a Lewis base, are present in these solutions. It was concluded[1] on the basis of infrared evidence that species II may exist in a form in which the sixth coordination site of the vanadium atom trans to the vanadyl oxygen is vacant or in a form where the sulfur atom of the dithiophosphinate, which is displaced by the ligand L, occupies this coordination site. Furthermore, the relative orientation of the monodentate ligands in species III was not ascertained. At very high concentrations of Lewis base, the dithiophosphinate ligands are completely displaced from the first coordination sphere of the vanadyl ion.[1] The enthalpy of reaction 1 was determined from the relative intensities of the ESR[1,3] and optical absorptions[3] of species I and II.

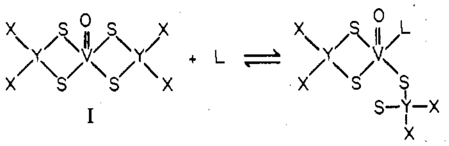
I II (1)

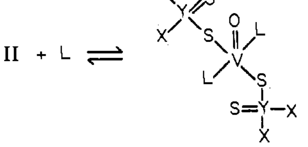
III (2)

The chelate displacement equilibria described above are in sharp contrast with the addition equilibria which have been suggested in the interaction of Lewis bases with vanadyl acetylacetonate,[4] eq 3 and 4. Experimental measurements of the interactions of other vanadyl complexes with Lewis bases have generally been interpreted in terms of reaction 3.[5]

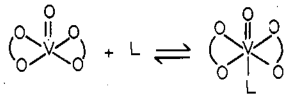
(3)

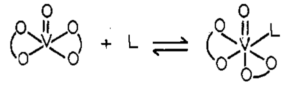
(4)

The transition metal complexes with dithioarsinate ligands[6-9] form a series of complexes which parallels the series of dithiophosphinate complexes.[1-3,10-12] The existing body of published work indicates that substitution of an arsenic atom for a phosphorus atom in what is effectively the second coordination sphere of the metal ion does not produce significant changes in the electronic properties of the metal complexes. The preparation and electronic and ESR spectra of bis(dimethyldithioarsinato)oxovanadium(IV) were reported[9,10] while the present work was in progress. The ESR spectra of $OV[S_2As(CH_3)_2]_2$ are different from those of $OV[S_2P(CH_3)_2]_2$[1-3,11,12] since ^{75}As has spin $^3/_2$ while ^{31}P has spin $^1/_2$. However, the magnitude of the isotropic ^{75}As hyperfine coupling indicates that the distribution of unpaired electron density in $OV[S_2As(CH_3)_2]_2$ is similar to that in $OV[S_2P(CH_3)_2]_2$. The isolation of the bis(pyridine) adduct of

---

* To whom correspondence should be addressed at the Physics Laboratory, University of Kent, Canterbury, Kent, England.